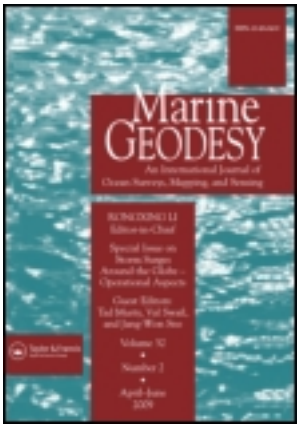

Marine Geodesy
Publication details, including instructions for authors and subscription information:
http://www.tandfonline.com/loi/umgd20

Airborne Gravity Surveys Over Taiwan Island and Strait, Kuroshio Current and South China Sea: Comparison of GPS and Gravity Accuracies at Different Flight Altitudes

Cheinway Hwang [a], Hsuan-Chang Shih [a], Yu-Shen Hsiao [a] & Chi-Hsun Huang [a]

[a] Department of Civil Engineering, National Chiao Tung University, Taiwan, Republic of China

Accepted author version posted online: 27 Mar 2012.Published online: 27 Aug 2012.

To cite this article: Cheinway Hwang, Hsuan-Chang Shih, Yu-Shen Hsiao & Chi-Hsun Huang (2012) Airborne Gravity Surveys Over Taiwan Island and Strait, Kuroshio Current and South China Sea: Comparison of GPS and Gravity Accuracies at Different Flight Altitudes, Marine Geodesy, 35:3, 287-305, DOI: 10.1080/01490419.2011.634962

To link to this article: http://dx.doi.org/10.1080/01490419.2011.634962

Marine Geodesy, 35:287–305, 2012

ISSN: 0149-0419 print / 1521-060X online
DOI: 10.1080/01490419.2011.634962

Taylor & Francis
Taylor & Francis Group

Airborne Gravity Surveys Over Taiwan Island and Strait, Kuroshio Current and South China Sea: Comparison of GPS and Gravity Accuracies at Different Flight Altitudes

CHEINWAY HWANG, HSUAN-CHANG SHIH, YU-SHEN HSIAO, AND CHI-HSUN HUANG

Department of Civil Engineering, National Chiao Tung University, Taiwan, Republic of China

We compare the accuracies of GPS and gravity observations obtained from three airborne gravity surveys over Taiwan Island at altitude 5000 m and over Kuroshio Current, Taiwan Strait, and Dongsha Atoll at altitude 1500 m. A kinematic network adjustment was used to determine the positions of the aircrafts. GPS positioning errors are at the decimeter-level, which are not entirely propagated to velocity and acceleration errors due to cancellation of long wavelength errors. Outliers are downweighted in the Gaussian filtering to improve the gravity accuracy, especially at altitude 1500 m. Compared with the upward-continued gravity, the gravity anomalies from the 1500-m surveys show a consistent accuracy of about 3 mgal; the accuracy from the 5000-m survey is degraded, especially over high mountains. The RMS crossover differences at 1500 m and 5000 m are all below 3 mgal, suggesting flight altitudes do not affect the crossover difference. Coherence analysis suggests that the spatial resolvable wavelengths of the airborne gravity range from 4 km (altitude 1500 m) to 6 km (altitude 5000 m).

Keywords Airborne gravity, Dongsha Atoll, filter, Kuroshio Current, Taiwan

1. Introduction

Gravity data are important for a number of applications (Torge 1989). Over inaccessible areas and oceans, a common tool for collecting gravity data is airborne gravimetry, which matches the need of Taiwan due to its rough terrain and vast oceans surrounding it. Worldwide results of airborne gravity surveys have been documented in several publications, for example, Wei and Schwarz (1998), Glennie and Schwarz (1999), Verdun et al. (2003), Forsberg et al. (2003), and Hwang et al. (2007). In the international earth science community, the region around Taiwan is an interesting and ideal place for geophysical and oceanographic studies in fields such as geoid modeling, mountain building, plate tectonics, earthquake mechanism, and ocean circulation. Recently, it has been realized that seismic tomography cannot fully explain the earth's interiors, and gravity data have become

Received 12 February 2011; accepted 29 September 2011.
Address correspondence to Cheinway Hwang, Department of Civil Engineering, National Chiao Tung University, 1001 Ta Hsueh Road, Hsinchu 300, Taiwan, ROC. E-mail: cheinway@mail.nctu.edu.tw; cheinway@gmail.com

increasingly important to assist seismic data in understanding the structure of the earth; see, for example, Xia et al. (1994), Masson et al. (2010), and Dove et al. (2010).

Around Taiwan, Hwang et al. (2007) has carried out the first airborne gravity survey at altitude 5000 m, and the resulting gravity data have been applied to modeling a Taiwan geoid and estimating Kuroshio Current velocities (Hwang et al., 2008), joint inversion of lithosphere structure (Masson et al., 2010), and vertical datum determination. Recently, more airborne gravity surveys around Taiwan were made over three areas: (1) the Kuroshio Current east of Taiwan, (2) the Taiwan Strait, and (3) Dongsha Atoll in the northern South China Sea. The field work and data processing were mainly carried out by the gravity team in National Chiao Tung University (NCTU). One major difference of these new surveys from the survey of Hwang et al. (2007) is the flight altitude: 1500 m (new surveys) versus 5000 m (Hwang et al. 2007). These three new surveys also overlap partially with the survey at altitude 5000 m in geographic coverage. In theory, with the same aircraft, flight speed, gravimeter and data reduction method, the airborne gravity at altitude 1500 m will contain higher spatial frequency information than the gravity at altitude 5000 m. However, this may not always be true because the flight condition at altitude 1500 m is, in general, different from that at altitude 5000 m. For example, a flight at altitude 1500 m has a higher chance of encountering clouds that make the aircraft experience large dynamics, which can degrade the Global Positioning System (GPS) accuracy. Other unknown reasons may also give rise to differences in the GPS positioning accuracies and gravity accuracies at altitudes 1500 m and 5000 m.

The objective of this paper is to present the gravity anomalies collected in the three airborne gravity surveys. Such gravity data will be of both regional and international interests for the scientific purposes discussed above. We will also analyze the accuracies of GPS positioning and gravity anomaly under the two different flight altitudes. Gravity accuracies over areas of different gravity variations will also be investigated. For all the airborne gravity surveys, the gravimeter used is a Lacoste & Romberg System II air/sea gravimeter (LCR 2002), and the aircrafts used are Beechcraft King Air 200 and 350 (depending on the availability; two aircrafts are used in one survey), with a Trimble 5700 GPS receiver onboard the aircrafts.

2. Airborne Gravity Surveys

2.1. Taiwan Island at Altitude 5000 m

The Taiwan Island airborne gravity survey was carried out at altitude 5000 m over the period of May 2004 to March 2005, and the result has been documented by Hwang et al. (2007). The analysis of the result from this survey presented in this paper is a revised version of Hwang et al. (2007). The goal of this project is to obtain evenly distributed gravity data over the entire Taiwan Island, especially over the Central Range of Taiwan, where ground gravity data are sparse. The field work lasted 43 days, with total flight hours of about 200. The numbers of survey lines in the north-south, east-west, northeast-southwest, and northwest-southeast directions are 64, 22, 10, and 6, respectively (Figure 1a). The cross-line spacing is 4.5 km for all survey lines, except the east-west lines, which are spaced at 20 km. The east-west lines are mainly for crossover analysis. The speed of flight is 306 km/hour relative to the ground. The gravity readings were recorded at one second interval (1-Hz), and this corresponds to an 85-m interval on the ground. For GPS positioning of the aircrafts, the GPS data sampling interval was also set to one second. Altogether, GPS data at seven

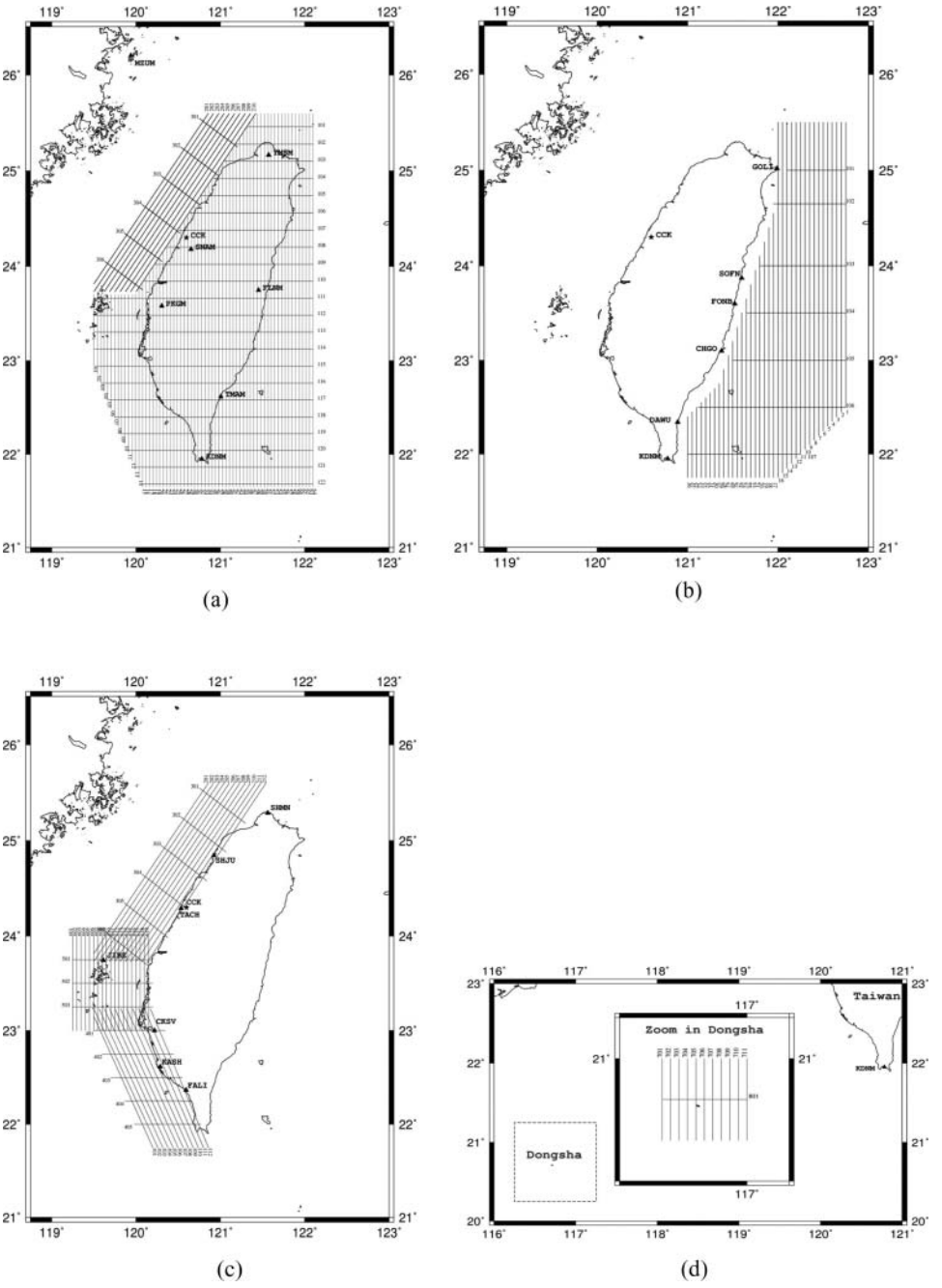

Figure 1. Survey lines of airborne gravity over (a) Taiwan Island, (b) Kuroshio Current, (c) Taiwan Strait and (d) Dongsha Atoll.

permanent GPS stations in Taiwan and one station (Figure 1a) in the Taichung airport (CCK in Figure 1a, all flights started here) were collected for GPS positioning.

2.2. Kuroshio Current at Altitude 1500 m

The Kuroshio Current airborne gravity survey was flown over the period of March 2006 to August 2008. This project aims to map the Kuroshio Current east of Taiwan by the combination of airborne gravity data, surface gravity data, and satellite altimetry data. The idea is to use the gravity data to compute an accurate geoid model over the Kuroshio Current east of Taiwan. With satellite altimetry data, the geostrophic currents over the Kuroshio Current can be determined. The resulting gravity will be also useful for the study of the plate dynamics in the collision zone of the Eurasia Plate and the Philippine Sea Plate. The Kuroshio Current survey contains 36 and 7 lines in the north-south and east-west directions, respectively (Figure 1b). The cross-line spacing is 5 km for all north-south lines and 60 km for east-west lines. All lines are distributed over the Kuroshio Current east of Taiwan. Unlike the survey over the Taiwan Island, the flight altitude over the Kuroshio Current was set to 1500 m to increase the spatial resolution of gravity data. The speed of flight is 280 km/hour with 1-Hz sampling rate, corresponding to a 77 m interval on the ground. The same GPS tracking network as in the Taiwan Island survey was used.

2.3. Taiwan Strait and Dongsha Atoll (Northern South China Sea) at Altitude 1500 m

The Taiwan Strait and Dongsha Atoll (in northern South China Sea) are typical shallow-water areas, defined as waters with a depth $<$500 m. In this area, the existing shipborne gravity data were sparsely distributed and collected mainly by research vessels studying marine geophysics around Taiwan in the 1980s and 1990s (Hwang and Hsu 2008). Currently, altimeter-derived gravity is the most important source of gravity in the region. However, altimeter-derived gravity in shallow waters can be seriously degraded due to bad tidal correction, bad wet tropospheric correction, large sea surface variability, and contaminated altimeter waveforms (Deng et al. 2003; Hwang and Hsu 2008). Therefore, it is expected that the gravity data here can be improved by airborne gravimetry. This motivates the airborne gravity survey over the Taiwan Strait and Dongsha Atoll.

For this survey, the gravity values at altitude 1500 m over the Taiwan Strait and Dongsha Atoll were collected in 115-flight hours over 2008–2009. The ground spacings along the 54 north-south and 15 east-west lines are 5 and 25 km, respectively. The flight speed and the corresponding gravity sampling interval are 280 km/hour and 77 m, which are the same as those for the survey over the Kuroshio Current. Again, the GPS tracking network is the same as the one used in the other two surveys. Figures 1c and 1d show the survey lines over the Taiwan Strait and Dongsha Atoll, respectively. Due to logistics, we had only one east-west line over the Dongsha Atoll. Due to a political consideration (not to cross the central Taiwan Strait), the east-west lines over the Taiwan Strait are relatively short, making the filtering of the raw gravity and GPS data less effective compared to long survey lines.

3. Assessing Accuracies of GPS Positioning at Different Altitudes

The trajectories of the two Beechcraft King Air 200 and 350 aircrafts were determined by the Bernese 5.0 software (Beutler et al. 2004; Dach et al. 2007) using a kinematic network adjustment. That is, the kinematic baselines between the GPS tracking stations (Figure 1a) and the aircraft were formed first and then optimally adjusted to determine

Table 1
Averaged RMS differences from 20 GPS overlapping sessions of the Kuroshio and Taiwan Strait surveys at altitude 1500 m, and the Taiwan Island survey at altitude 5000 m

	(a) 1500 m		
	North	East	Vertical
Position (m)	0.137	0.268	0.421
Velocity ($m \cdot s^{-1}$)	0.0064	0.0081	0.0108
Acceleration (mgal)	93.88	74.53	906.28
	(b) 5000 m		
	North	East	Vertical
Position (m)	0.073	0.208	0.293
Velocity ($m \cdot s^{-1}$)	0.0003	0.0003	0.0013
Acceleration (mgal)	23.56	26.56	104.85

the coordinates of the aircraft (Hwang et al. 2007). The positions of the aircraft were then numerically differentiated to determine the aircraft's velocities and accelerations for the reduction of airborne gravity reading to gravity anomaly. Here, an accurate assessment of GPS-determined position, velocity, and acceleration is presented, with a motivation to see the relation between GPS accuracy and flight altitude. We selected ten sessions of GPS data from the Kuroshio Current and Taiwan Strait surveys (at altitude 1500 m) and ten sessions from the Taiwan Island survey (at altitude 5000 m) for the accuracy assessment. Each session lasted about four hours and was divided into two independently processing subsessions with a 30-minute overlap. Twenty overlapping sessions were formed and the tracks of the overlaps cover coastal plains, high mountains, and oceans.

Tables 1a and 1b list the average RMS differences in position, velocity, and acceleration from the 20 overlapping sessions (10 for each altitude) at altitudes 1500 m and 5000 m, respectively. The result in Table 1b is directly from Hwang et al. (2007). The overall positioning error is of the order of decimeter, with the vertical component being the largest. In general, the north component has a better accuracy than the east component, but there are exceptions. The overlapping differences in velocity and acceleration at altitude 1500 m are larger than those at altitude 5000 m. The flights at altitude 1500 m will encounter more turbulences than the flights at 5000 m because of the structure of the atmosphere. Because the air at 1500 m is denser than the air at 5000 m and the former has a higher water concentration, the aircraft will experience larger dynamics at altitude 1500 m. Also, GPS signals at altitude 1500 m contain more atmospheric influence such as tropospheric delays than the case at 5000 m. These lead to larger errors in GPS positioning, and consequently velocity and acceleration at altitude 1500 m.

From the result of Table 1, it appears that the long wavelength positioning errors do not propagate into the errors in velocity and acceleration. This is explained using the finite-difference formulae

$$\begin{aligned} \mathrm{v}_z &\approx \frac{\Delta z}{\Delta t} \\ \mathrm{a}_z &\approx \frac{\Delta v_z}{\Delta t} \end{aligned} \tag{1}$$

where v_z, and a_z are the vertical velocity and acceleration, Δz and Δv_z are the differences between two along-track, successive vertical positions and velocities, and $\Delta t = 1$ **s** (the sampling interval for the airborne gravity surveys in this paper). Ignoring the correlations between successive positions, the standard errors of vertical velocity and acceleration can be approximated as

$$\sigma_{v_z} \approx \frac{\sqrt{2}\sigma_z}{\Delta t}$$
$$\sigma_{a_z} \approx \frac{2\sigma_z}{\Delta t^2} \tag{2}$$

By this approximation, a 0.10 m-positioning error will lead to a velocity and an acceleration error of 0.14 ms^{-1} and 0.20 ms^{-2} (20000 mgal), respectively. However, the RMS differences (roughly $\sqrt{2}$ times of the standard error) in Table 1 are much smaller than the standard errors predicted by Eq. (2). This suggests that the numerical differentiations of airplane positions have reduced the long wavelength GPS positioning errors.

4. Reduction of Airborne Gravity Data and Result

4.1. Downweighting Outliers and Filtering

The method of gravity reduction used in the paper is largely based on the work of Hwang et al. (2006). However, an improved procedure of data reduction was used in this paper, especially in outlier detection and filtering. An outlier is an observation that is numerically distant from the rest of the data (Barnett and Lewis 1994) and will lead to a serious consequence in data processing and interpretation. In an airborne gravity survey, outliers can be caused by cycle slips in GPS phase data, air turbulence, electronic problem of the gravimeter, and so forth. There are several methods to deal with outliers in airborne gravimetry. For example, Alberts (2009) used a robust estimation approach to remove outliers; the method is known as M-estimation (Huber 1981). In this paper, we use the following procedure to remove outliers in gravity data. The raw gravity data were first filtered by the Gaussian filter using a filter window twice as wide as that used to produce the final gravity. The Gaussian filter we used is developed by the NCTU team (the team collecting the airborne gravity data in this paper) and is documented in Hwang et al. (2006). This filter is being continuously updated to achieve the optimal result in this paper. The standard deviation (sigma) of the differences between raw and filtered data was then computed. A raw gravity observation whose difference with the filtered value exceeds three times of the standard deviation is considered an outlier, and the corresponding observation was downweighted as

$$w'_t = w_t \cdot \begin{cases} \exp(\frac{-|\delta|}{3\sigma}) & \text{if } |\delta| > 3\sigma \\ 1 & \text{if } |\delta| \leq 3\sigma \end{cases} \tag{3}$$

where w'_t is the new weight, w_t the original weight, σ the standard deviation and δ the difference between the raw value and filtered value. In Eq. (3), σ is computed as the standard deviation of the differences between raw and filtered gravity values for each survey line. This is the so-called three sigma rule of downweighting. An outlier with a larger difference will receive a smaller weight. As an example, Figure 2 shows the raw gravity anomalies and outliers along Line 17 (Figure 1b) of the Kuroshio airborne gravity

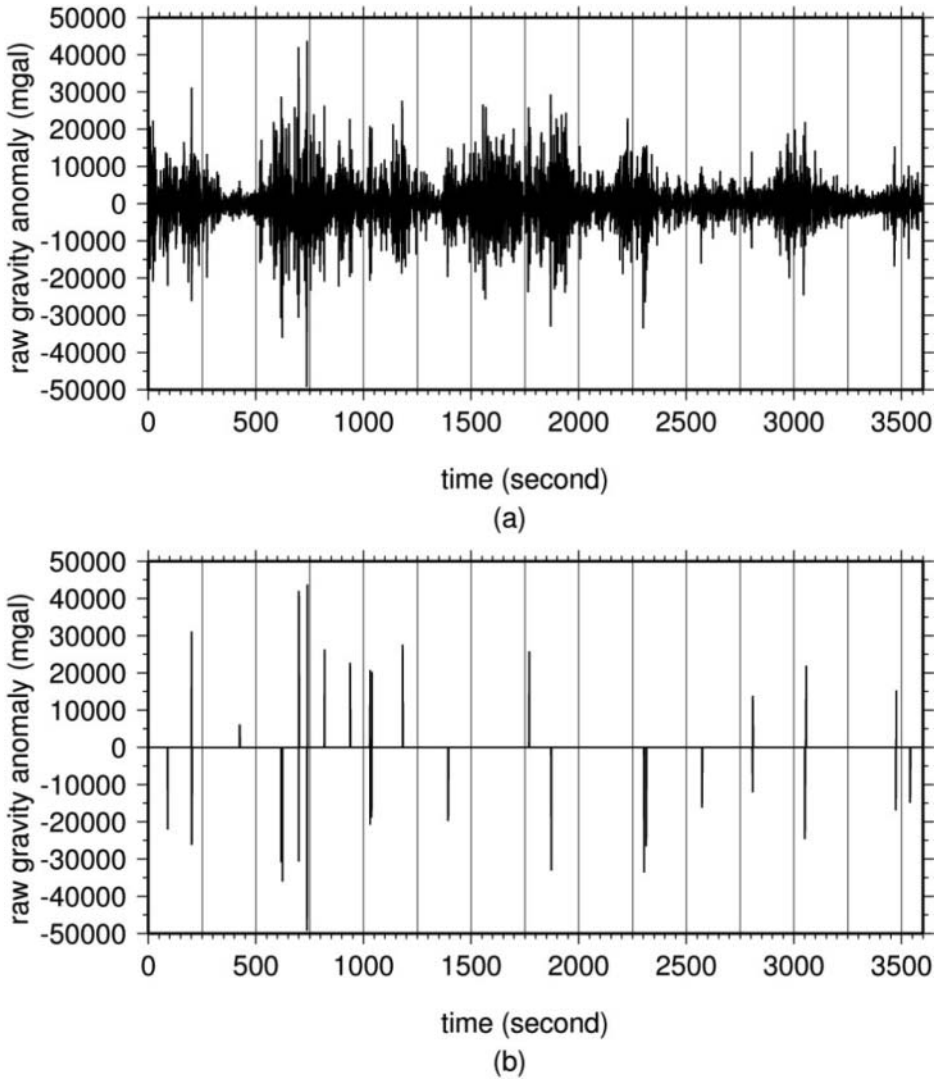

Figure 2. Raw gravity anomalies (top) and outliers along Line 17 of the Kuroshio Current campaign.

survey. The outliers are seen in the raw data as spikes. With new weights, a Gaussian filter was again used to obtain the filtered gravity values, and the outlier detection-filtering was iterated until no outlier was found. For outlier detection, a filter window about 10–20 seconds is appropriate, depending on the duration of turbulence in the flight.

In addition to the Gaussian filer, we also experimented with two other filters: Butterworth filter (Buttkus 2000) and the Hilbert-Huang Transform (HHT) filter. A case study of airborne gravity using the Butterworth filter can be found in Olesen (2003), who provided us with this filter. The HHT filter was documented by Huang et al. (1998), and the software was made available to us by a vendor in Taiwan. As an example of filter, Figure 3 shows the filtered gravity anomalies along Line 17 based on the Gaussian, Butterworth, and HHT filters. The statistics of the differences between the upward-continued gravity and the filtered

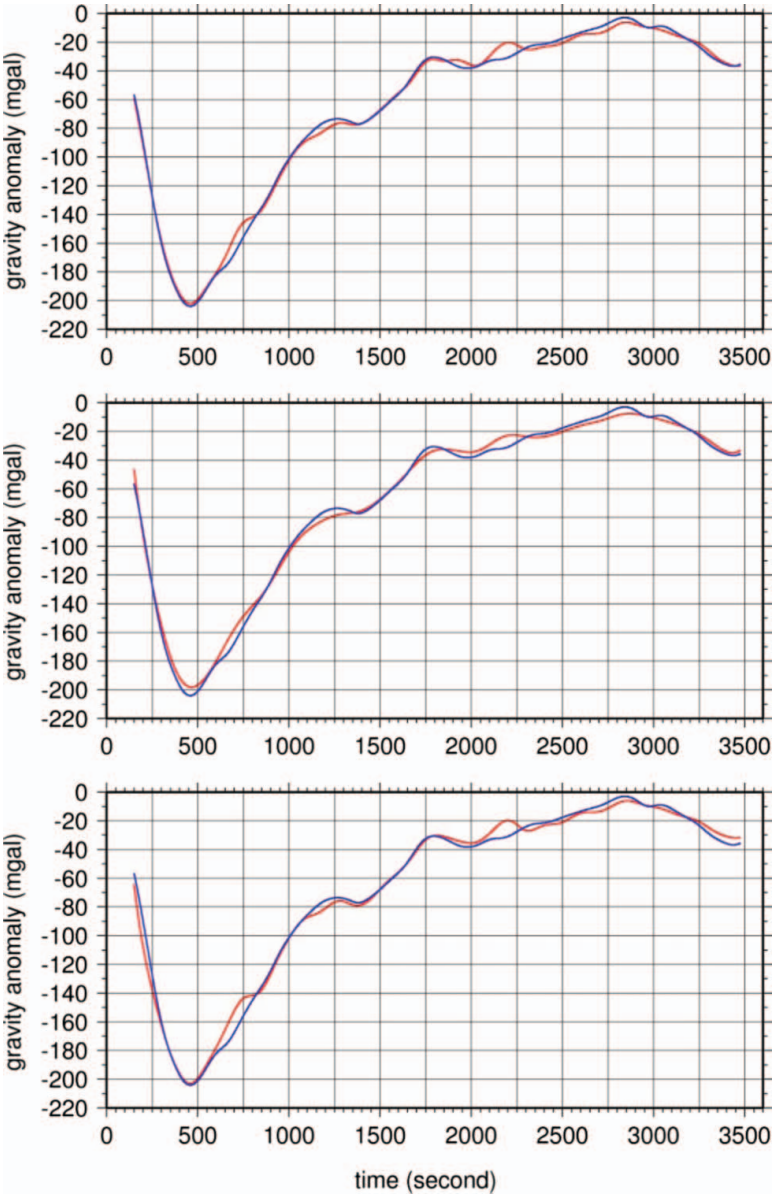

Figure 3. Filtered gravity anomalies using the (a) Gaussian (b) Butterworth (c) and HHT filters from the corrected gravity data along Line 17. (Figure available in color online.)

ones (based on a 150-s filter width for all filters) along Line 17 are summarized in Table 2. Table 2 suggests that a filter must also have the function of outlier detection to achieve a best result: if the outliers are not removed, the RMS difference is 3.56 mgal, which is larger than 2.87 mgal when outliers are downweighted. Although the best result in Table 2 is from the Gaussian filter (with the function of outlier detection), the Butterworth and HHT filters may do equally well as the Gaussian filter, provided that the former two filters available to us can be optimized in the source code, and have the function of outlier handling.

Table 2
Statistics of differences between the upward-continued surface gravity and the airborne gravity filtered by the Gaussian, Butterworth and HHT filters along Line 17 from the Kuroshio Current survey (unit: mgal)

Filter type	Min	Max	Mean	STD	RMS
Gaussian	−5.99	11.84	0.10	3.56	3.56
Butterworth	−5.72	10.33	0.40	3.67	3.70
HHT	−17.91	15.14	0.08	4.96	4.96
Gaussian with outlier detection	−7.31	10.92	0.03	2.87	2.87

4.2. Free-Air Gravity Anomalies at Flight Altitudes

Figure 4 shows the free-air gravity anomalies obtained from the Taiwan Island, Kuroshio Current, Taiwan Strait, and Dongsha Atoll airborne gravity surveys, respectively. The gravity anomalies are highly correlated with terrain and ocean bottom topography. The maximum gravity anomaly of about 250 mgal is found over the Central Range of Taiwan, and the minimum value of about −200 mgal is over the trenches east of Taiwan, which is partially covered by the 5000-m and 1500-m surveys. As expected, gravity anomalies from the 5000-m survey are in general smoother and smaller than the values from the 1500-m survey because the former is at a higher altitude that attenuates more gravity signal than the latter. Also, the gravity anomalies over the Ludao and Lanyu Islands off the southeastern coast of Taiwan are larger in comparison to the ambient gravity values. These gravity highs are due to the mass of the two islands form during volcanic eruptions. Figure 4 shows that, the 1500-m survey delivers more pronounced gravity signal than the 5000-m survey over the two islands.

The gravity anomalies over the Taiwan Strait vary from −30 to 40 mgal. Relatively large, positive gravity anomalies are found over the Penghu Island (at about 23.5° N, 119.5° E) in the Taiwan Strait, and such gravity highs extend to the western coastal Taiwan. This stretch of gravity highs is associated with the Pekang Basement High. It is expected that airborne gravity anomalies in the Taiwan Strait from this paper can improve the estimation of Moho depth (Hsieh et al. 2010). Over the Dongsha Atoll, the circular coverage of the gravity highs roughly agrees with the circular boundary of this atoll, which is a seamount in the northern South China Sea (Xia et al. 1994; Tsai et al. 2004). The alternating gravity values over this atoll, from negative values around Dongsha's flank to positive values on Dongsha's center, are typical for a seamount and are commonly seen in gravity anomalies derived from satellite altimetry (Hwang et al. 2002). However, the airborne gravity over the Dongsha Atoll contains a higher frequency gravity signal than that from satellite altimetry. As such, the former can be used to assess the latter, especially when an improved method of gravity derivation from altimetry is to be evaluated.

5. Accuracies and Spatial Resolutions of Airborne Gravity Data at Different Altitudes

5.1. Comparison with Upward-Continued Gravity

The hardware of GPS and gravimeter for the three airborne surveys are the same, but the flight altitudes are different (1500 m and 5000 m). This gives an opportunity to investigate

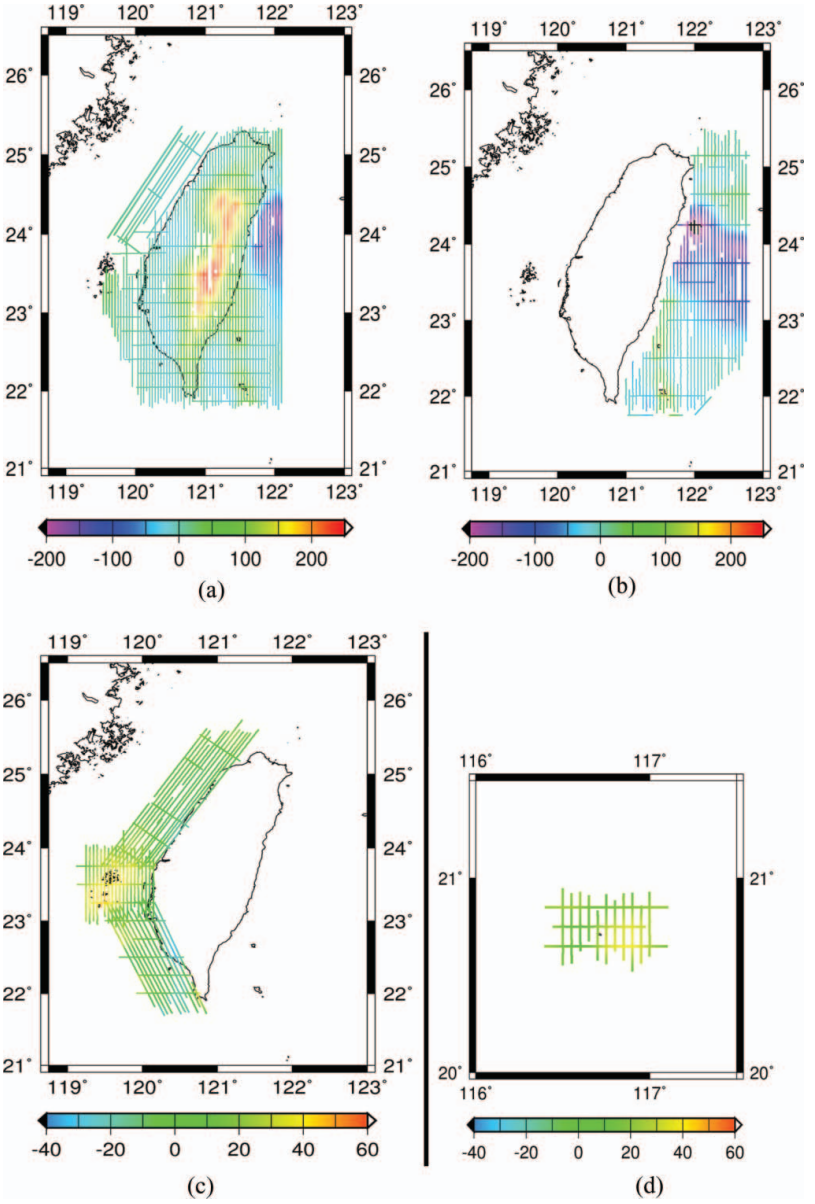

Figure 4. Free-air gravity anomalies obtained from the (a) Taiwan Island, (b) Kuroshio Current, (c) Taiwan Strait and (d) Dongsha Atoll airborne gravity surveys (Unit: mgal). (Figure available in color online.)

the relationship between gravity accuracy and flight altitude. Our investigation begins with the comparison between the airborne gravity anomalies and upward-continued surface gravity anomalies. We used the same surface gravity anomalies and the same method of upward continuation presented in Hwang et al. (2007). For the upward continuation, the long wavelength gravity anomalies of EGM08 (Pavlis et al. 2008) up to 720° were first

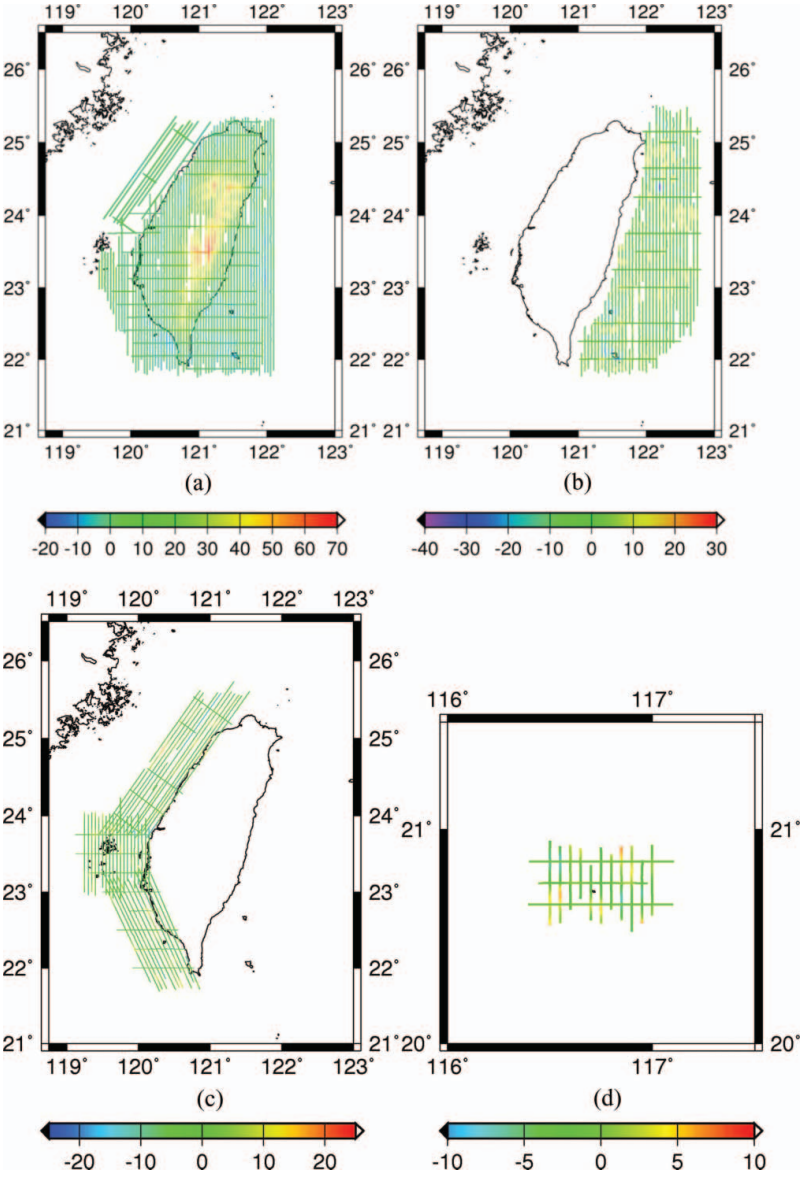

Figure 5. Differences between the upward continued and the airborne gravity anomalies over (a) the Taiwan Island, (b) Kuroshio Current, (c) Taiwan Strait and (d) Dongsha Atoll (Unit: mgal). (Figure available in color online.)

removed from the surface gravity anomalies. The residual gravity anomalies were then gridded and upward-continued to the flight altitude using Fourier transform. The long wavelength gravity anomalies due to EGM08 at the flight altitude were then restored to obtain the final gravity anomalies.

Figure 5 shows the differences between the upward-continued and the airborne gravity anomalies. The statistics of the differences are summarized in Table 3. Most of the large

Table 3
Statistics of differences between the upward-continued surface gravity and the airborne gravity (unit: mgal)

Airborne surveys	Min	Max	Mean	STD	RMS
Taiwan Island	−11.497	69.908	9.183	12.099	15.189
Kuroshio Current	−32.551	17.932	−0.215	3.788	3.794
Taiwan Strait	−14.093	16.080	−0.020	3.710	3.710
Dongsha Atoll	−6.998	6.813	−0.347	2.397	2.420

differences occur over high mountains of Taiwan, and few over deep trenches east of Taiwan. The dominating causes of these large differences are as follows:

(1) Errors in airborne gravity measurements, for example, the scattering large differences along four north-south lines east of Taiwan.
(2) Low data density and quality in surface gravity anomalies. For example, relatively large differences occur at the immediate vicinity of all coasts, the Central Range, and the waters northwest of Taiwan because here the surface gravity data densities are relatively low, making the upward-continued gravity values less accurate.
(3) Large gravity gradients over areas of rough gravity fields. In this case, the attenuated gravity values at the flight altitudes will fail to capture the high-frequency gravity variations.

The gravity fields over the Central Range (low surface data density) and over the ocean trenches east of Taiwan (high surface data density) are equally rough, but large differences are found only over the Central Range. This suggests that the differences in Figure 5 are largely affected by surface gravity data density, rather than errors in the airborne gravity measurements. In Figure 5, some large differences occur along a survey line and its neighboring lines. This is due to some improperly upward continued gravity values that affect not just one line but also multiple lines. Based on our logging data, some of the large differences are caused by the unstable flight attitudes at the beginning of the lines and the turbulences during the flights.

5.2. Crossover difference of gravity

The theory of crossover analysis is based on the concept that the gravity anomalies from two intersecting survey lines should be the same. The use of gravity anomaly can avoid height-dependent error because gravity anomaly is less sensitive to height (within a certain range) compared to absolute gravity value. The linear interpolation is necessary to determine the crossover location of the intersecting lines and the corresponding gravity anomalies. Figures 6 and 7 show the spatial distribution of the crossover differences from the three airborne gravity surveys. The numbers of crossover points are 512, 200, 171, and 30 in the Taiwan Island, Kuroshio Current, Taiwan Strait, and Dongsha Atoll surveys, respectively. The statistics of crossover differences (before crossover adjustment) are summarized in Table 4.

Due to poor GPS data and turbulences during the flight, some crossover differences are excessively large, and a crossover difference larger than 15 mgal is considered an outlier and not used for the subsequent analyses. The distribution of crossover differences

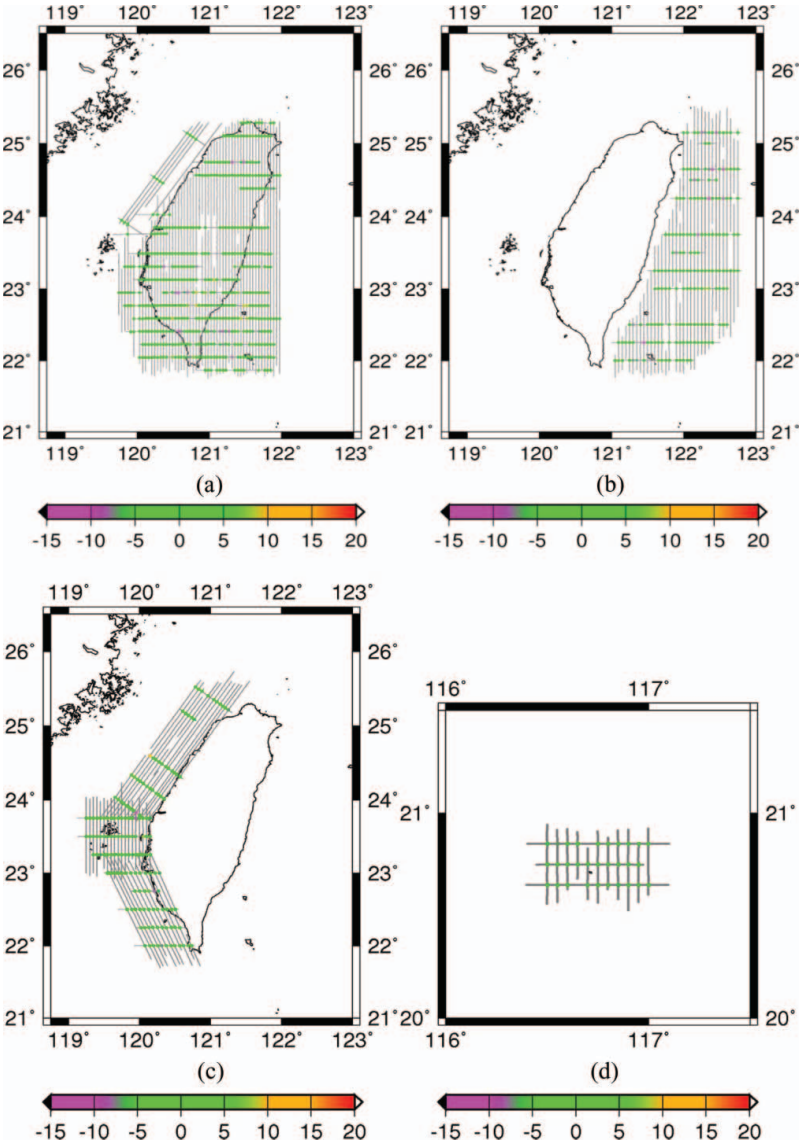

Figure 6. Spatial distributions of the crossover differences from the three airborne gravity surveys in Taiwan (Unit: mgal). (Figure available in color online.)

approximately follows the normal distribution (Figure 7), suggesting that these crossover differences are largely due to random noises. Similar to the pattern of differences between upward-continued and airborne gravity anomalies (Figure 5), large crossover differences occur over high mountains. Crossover difference is partly caused by interpolation error, especially over areas with a rough gravity field. Because the Eötvös gravity effect is the largest in the east-west direction, under the same velocity accuracy the east-west lines are likely to contain larger errors in gravity and in turn result in larger crossover differences (Hwang et al. 2007). Therefore, some of the large crossover differences may be caused

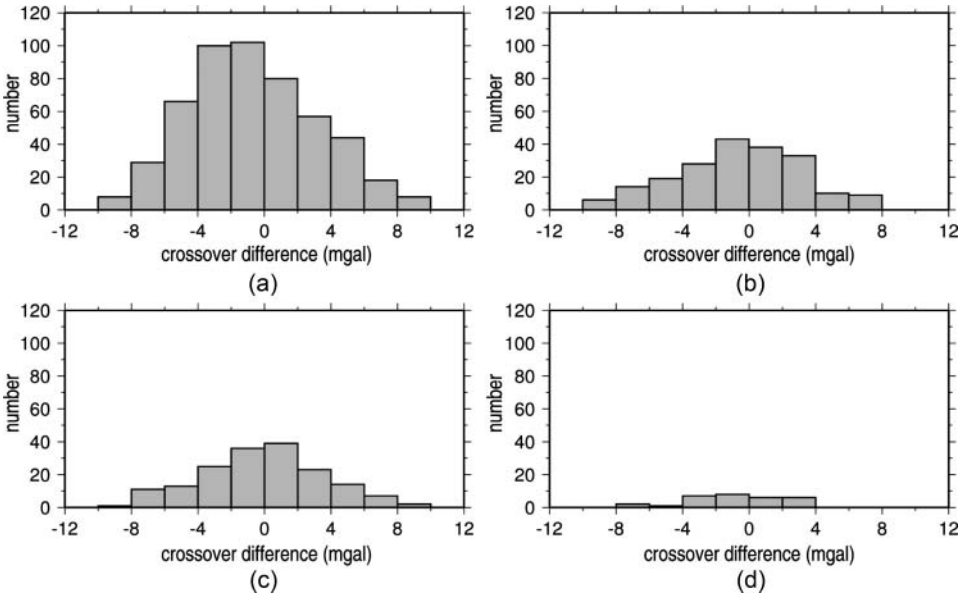

Figure 7. Histograms of the crossover differences from the three airborne gravity surveys in Taiwan.

Table 4
Statistics of crossover differences of the airborne gravity anomalies before crossover adjustment (unit: mgal)

Airborne surveys	Min	Max	Mean	STD	RMS
Taiwan Island	−8.751	8.898	−0.685	3.844	3.901
Kuroshio Current	−9.554	7.772	−0.6060	3.809	3.848
Taiwan Strait	−9.478	9.586	−0.087	3.614	3.604
Dongsha Atoll	−7.000	3.981	−0.588	2.839	2.853

Table 5
Statistics of crossover differences of the airborne gravity anomalies in eastern Taiwan with overlapped flights (unit: mgal)

Airborne surveys	Min	Max	Mean	STD	RMS
Taiwan Island	−8.480	8.740	−0.628	4.157	4.189
Kuroshio Current	−9.280	7.130	−0.137	3.363	3.349

Table 6
Statistics of crossover differences of the airborne gravity anomalies over Taiwan Strait with overlapped flights (unit: mgal)

Airborne surveys	Min	Max	Mean	STD	RMS
Taiwan Island	−8.370	8.630	−0.750	3.253	3.327
Taiwan Strait	−9.480	9.590	−0.069	3.613	3.602

by poor horizontal velocity accuracy along the east-west lines. However, spurious gravity values caused by poor GPS positioning, turbulences, and instrument problems will still be the dominating contributors to the large crossover differences. In addition, there two areas with overlapped flights of airborne gravity at altitudes 5000 and 1500 m: (1) a narrow north-south band from the east coast to tens of km offshore in eastern Taiwan (over the Kuroshio Current) and (2) the eastern part of Taiwan Strait. The statistics of crossover differences in the two overlapped areas are summarized in Tables 5 and 6, respectively. In the first overlapped area (Table 5), the standard deviation of 4.157 mgal from the Taiwan Island survey (5000 m) is approximately 0.8 mgal larger than that from the Kuroshio Current survey (1500 m). However, in the second overlapped area, the crossover difference from the survey at altitude 1500 m is smaller than that from the survey at altitude 5000 m. However, in general the crossover differences from the two surveys at different altitudes are consistent at 1 mgal.

In order to reduce possible systematic errors, we performed a crossover adjustment using the weighted constraint method developed by Hwang et al. (2006). In the adjustment, gravity anomalies on a survey line are assumed to be corrupted by a bias. A bias along a survey line could be caused by improper base readings, "tare" in a sudden turbulence, problems in GPS results, and so forth. Since the reported drift of the LCR air-sea gravimeter is less than 3 mgal per month and each session of flight lasts only about 4 hour, the effect of gravimeter drift is not modeled. In order to eliminate the rank defect in the adjustment, at least one survey line must be held fixed. Those gravity anomalies along survey lines that agree very well with upward-continued surface gravity anomalies were held fixed in the adjustment. Also, survey lines with less than 2 crossover differences are not adjusted. Table 7 shows the statistics of the crossover differences after the crossover adjustment. The adjustment has reduced the RMS crossover differences given in Table 4. The biases are about few mgal, and there is no specific pattern in the distribution of the biases. Assuming that the RMS difference after the adjustment is solely due to random noises, Table 7 suggests that the averaged standard errors of "point" airborne gravity anomalies collected in the Taiwan Island, Kuroshio Current, Taiwan Strait, and Dongsha Atoll airborne gravity

Table 7
Statistics of crossover differences of the airborne gravity anomalies after crossover adjustment (unit: mgal)

Airborne surveys	Min	Max	Mean	STD	RMS
Taiwan Island	−7.560	8.386	0.000	2.794	2.792
Kuroshio Current	−6.883	8.555	0.000	2.681	2.675
Taiwan Strait	−8.787	7.745	0.000	2.580	2.573
Dongsha Atoll	−6.314	5.424	−0.092	2.699	2.655

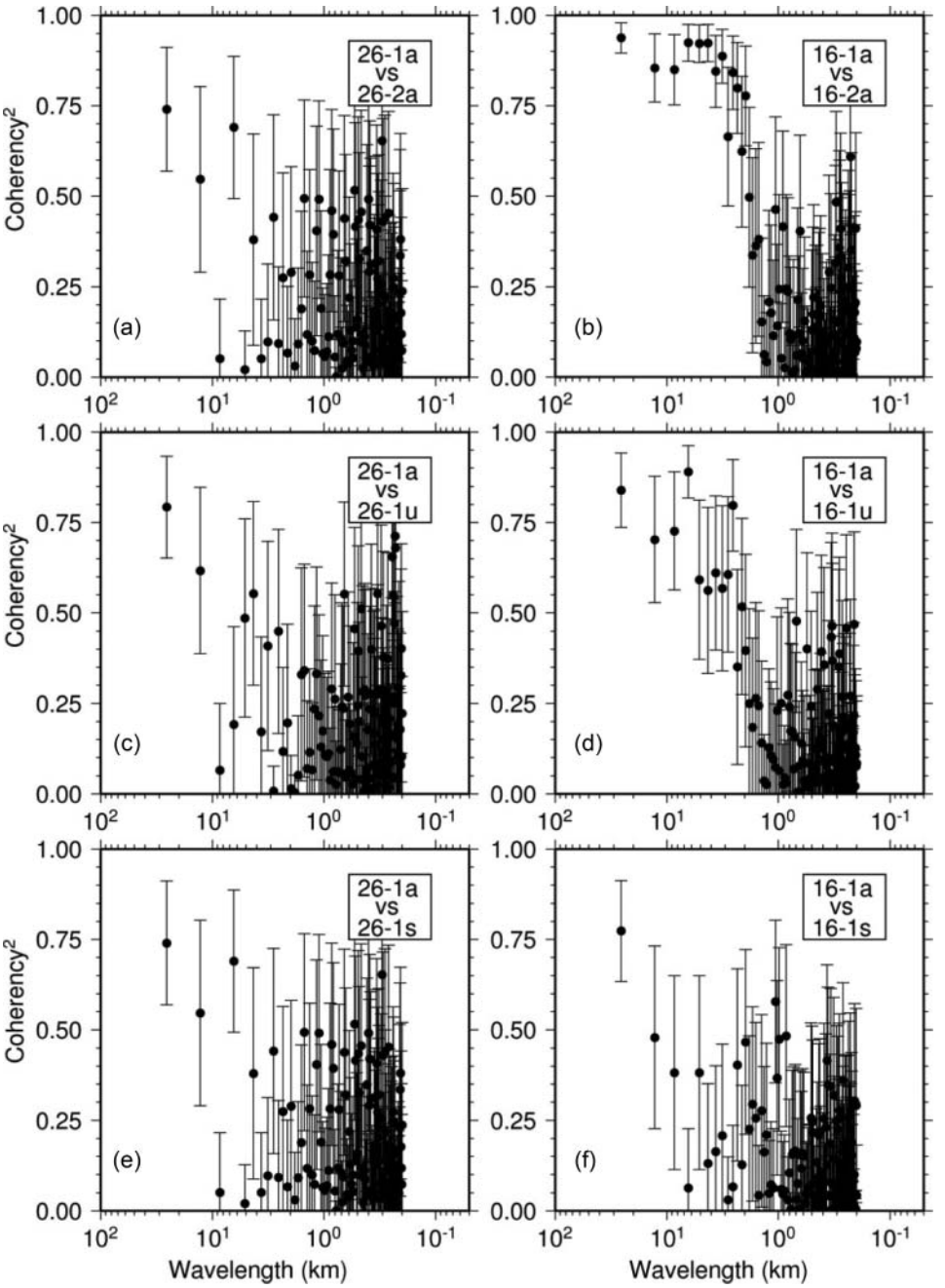

Figure 8. Squared coherences and error estimated (vertical bars) from repeated lines at different wavelengths.

surveys are about 1.97, 1.90, 1.82, and 1.88 mgal, respectively (the standard error is obtained by dividing the RMS difference by $\sqrt{2}$).

5.3. Along-Track Spatial Resolution of Gravity from Coherence Analysis

Many factors will affect the along-track spatial resolution of airborne gravity, for example, GPS positioning, weather condition at the flight time, and the gravimeter performance (Hwang et al. 2007). The spatial resolution also will depend on the width of the filter applied to the raw gravity and GPS data. In this paper, we used a Gaussian filter at a width of 150 s. The filtering was carried out as a numerical convolution between the Gaussian weight function and the raw data (Hwang et al. 2006). It will be useful to quantify the along-track spatial resolution of the airborne gravity filtered in this way. Here we follow the idea of coherence analysis of along-track altimeter sea surface height measurements given by Yale et al. (1995). Because parts of Line 16 over the Kuroshio Current at altitude 1500 m (Figure 1b) and Line 26 over Taiwan Island at altitude 5000 m (Figure 1a) were flown twice, we carried out a coherence analysis for such repeated measurements to estimate the resolvable wavelengths. For comparison, for each line we computed the squared coherences between airborne gravity and upward-continued gravity, and between airborne gravity and surface gravity. The squared coherence at frequency ω (wavelength $= 1/\omega$) between gravity measurements from two realizations x and y is defined as (Bendat and Piersol 2000):

$$\gamma_{xy}^2(\omega) = \frac{\left|S_{xy}(\omega)\right|^2}{S_{xx}(\omega) \cdot S_{yy}(\omega)}, \quad \text{with } 0 \le \gamma_{xy}^2 \le 1 \tag{4}$$

where S_{xy} is the cross spectral density between x and y, and S_{xx} and S_{yy} are the auto spectral densities of x and y, respectively. The independent variable for x and y can be time (t) or along-track distance (d), and the transformation between them is $d = vt$, where v is the speed of aircraft. The gravity signal components from x and y at a wavelength $1/\omega$ are said to be coherent if $\gamma_{xy}^2(\omega) \ge 0.5$, and this component is resolvable from any realization of the measuring process (in our case, airborne gravity measurement).

Figure 8 shows the squared coherences from the coherence analysis. In Figure 8, the numbers 16 and 26 indicate the survey lines, -1 and -2 are the first and second (repeated) flights; a, u, and s signify the airborne, upward-continued, and surface gravity, respectively. In general, the coherences for Line 16 are larger than those for Line 26. For Line 16 and for the case of airborne-airborne values, the coherence is larger than 0.5 for wavelengths larger than 4 km, and this suggests that at altitude 1500 m the minimum resolvable spatial wavelength is about 4 km, which is larger than the theoretical resolvable wavelength of 1 km (Hwang et al., 2007) due to measurement errors. Using the same reasoning for Line 26 (airborne-airborne), the minimum resolvable spatial wavelength at altitude 5000 m is about 6 km. All coherences in the cases of airborne-upward continued and airborne-surface are smaller than the coherences in the case of airborne-airborne, and such coherences for Line 16 are in general larger than the coherences for Line 26. This analysis shows that a low flight altitude is preferred over a high one in order to better resolve short wavelength gravity signals.

6. Conclusions

This paper presents the results of three airborne gravity surveys at altitudes 1500 m and 5000 m around Taiwan and South China Sea. The result for the survey at altitude 5000 m

in this paper is a revised one over the result of Hwang et al. (2007). The gravity data from the three surveys will enhance the current gravity database of Taiwan, which is largely based on satellite altimetry and terrestrial measurements. The enhanced gravity database is expected to improve a number of applications around Taiwan. Examples of applications are (1) modeling a regional geoid for height modernization in Taiwan, (2) understanding of the dynamics of collision between the Philippine Sea Plate and the Eurasia Plate, (3) understanding the isostasy over Taiwan, where mountain building is still ongoing, and (4) understanding the lithospheric structure of Taiwan for earthquake mechanism study. A summary from the three airborne gravity surveys is:

(1) GPS kinematic positioning errors are at the decimeter-level. Such errors are not entirely translated to velocity and acceleration errors due to cancellation of long wavelength errors. The positioning accuracy at 5000 m is better than that at 1500 m due to more stable flights (Table 1).
(2) Outliers should be handled with care in the filtering of raw airborne gravity to improve the gravity accuracy, especially at a lower altitude.
(3) Compared with the upward-continued gravity, the gravity anomalies from all the two 1500-m surveys show a consistent accuracy of about 3 mgal (Table 3); the accuracy from the 5000-m survey is degraded, especially over high mountains.
(4) The RMS crossover differences at 1500 m and 5000 m are all below 3 mgal (Table 4), suggesting flight altitudes do not affect the crossover difference (however, outliers must be removed for such a conclusion).
(5) Coherence analyses (Figure 8) suggest that the spatial resolvable wavelengths (defined as wavelengths with squared coherence >0.5) of the airborne gravity range from 4 km (altitude 1500 m) to 6 km (altitude 5000 m).

Acknowledgements

This is a five-year project sponsored by the Ministry of the Interior and the National Science Council, Taiwan, ROC (grant no. 97-2221-E-009-130-MY). We are grateful to the pilots from the National Airborne Service Corps., MOI, for the flexible adjustments of flights to complete this project.

References

Alberts, B. A. 2009. *Regional gravity field modeling using airborne gravity data*. Ph.D. thesis, Delft Institute of Earth Observation and Space Systems, Delft University of Technology, Netherlands.

Barnett, V., and T. Lewis. 1994. *Outliers in statistical data,* 3rd edition. New York: Wiley.

Bendat, J., and A. G. Piersol. 2000. *Random data: Analysis and measurement procedures*. Hanover: Wiley-Interscience.

Beutler, G., H. Bock, E. Brockmann, R. Dach, P. Fridez, W. Gurtner, H. Habrich, U. Hugentobler, D. Ineichen, M. Meindl, L. Mervare, M. Rothacher, S. Schaer, T. Springer, C. Urschl, and R. Weber. 2004. Bernese GPS Software Version 5.0 DRAFT, Astronomical Institute University of Bern, Switzerland.

Buttkus, B. 2000. *Spectral analysis and filter theory in applied geophysics*. Berlin: Springer.

Dach, R., U. Hugentobler, P. Fridez, and M. Meindl. 2007. User Manual of the Bernese GPS Software, Version 5.0, Astronomical Institute, University of Bern, Switzerland.

Deng, X., W. Featherstone, C. Hwang, and P. Berry. 2003. Waveform retracking of ERS-1. *Mar. Geod.* 25:189–204.

Dove, D., B. Coakley, J. Hopper, and Y. Kristoffersen. 2010. Bathymetry, controlled source seismic and gravity observations of the Mendeleev ridge; implications for ridge structure, origin, and regional tectonics. *Geophys. J. Int.* 183(2):481–502.

Forsberg, R., A. V. Olesen, K. Keller, and M. Moller. 2003. Airborne gravity survey of sea areas around Greenland and Svalbard. Technical Reports of National Survey and Cadastre, 18, Copenhagen, Denmark.

Glennie, C., and K. P. Schwarz. 1999. A comparison and analysis of airborne gravimetry results from two strapdown inertial/DGPS systems. *J. Geod.* 73:311–321.

Hsieh, H. H., H. Y. Yuan, and M. H. Shih. 2010. Moho depth derived from gravity data in the Taiwan Strait Area. *Terr. Atmos. Ocean. Sci.* 21:235–241.

Huang, N. E., Z. Shen, S. R. Long, M. C. Wu, H. H. Shih, Q. Zheng, N. C. Yen, C. C. Tung, and H. H. Liu. 1998. The empirical mode decomposition and the Hilbert spectrum for nonlinear and non-stationary time series analysis. *Proc. Roy. Soc. Lond.* A454:903–995.

Huber, P. H. 1981. *Robust statistics*. New York: Wiley.

Hwang, C., H. Y. Hsu, and R. J. Jang. 2002. Global mean sea surface and marine gravity anomaly from multi-satellite altimetry: applications of deflection-geoid and inverse Vening Meinesz formulae. *J. Geod.* 76:407–418.

Hwang, C., Y. S. Hsiao, and H. C. Shih. 2006. Data reduction in scalar airborne gravimetry: Theory, computer package and case study in Taiwan. *Comput. Geosci.* 32:1573–1584.

Hwang, C., Y. S. Hsiao, H. C. Shih, M. Yang, K. H. Chen, R. Forsberg, and A. V. Olesen. 2007. Geodetic and geophysical results from a Taiwan airborne gravity survey: Data reduction and accuracy assessment. *J. Geophys. Res.* 112(B10):B04407. doi: 10.1029/2005JB004220.

Hwang, C., and H. Y. Hsu. 2008. Shallow-water gravity anomalies from satellite altimetry: Case studies in the East China Sea and Taiwan Strait. *J. Chin. Inst. Eng.* 31:841–851.

Hwang, C., H. C. Shih, J. Y. Guo, and Y. S. Hsiao. 2008. Zonal and meridional ocean currents at TOPEX/Poseidon and JASON-1 crossovers around Taiwan: Error analysis and limitation. *Terr. Atmos. Ocean. Sci.* 19:151–162.

LCR. 2002. *Graviton-EG user's manual*. Austin: Lacoste &Romberg Inc.

Masson, F., M. Mouyen, C. Hwang, Y. M. Wu, M. Lehujeur, F. Ponton, and C. Dorbath. 2010. Lithospheric structure of Taiwan from gravity modeling and sequential inversion of seismological and gravity data. *Tectonophysics*, doi: 10.10161/jtecto.2012.04.012.

Olesen, A. V. 2003. Improved airborne scalar gravimetry for regional gravity filed mapping and geoid determination. Tech. Rep. No. 24, National Survey and Cadastre-Denmark, Copenhagen, Denmark.

Pavlis, N. K., S. A. Holmes, S. C. Kenyon, and J. K. Factor. 2008. An earth gravitational model to degree 2160: EGM2008. Presented at the 2008 European Geosciences Union General Assembly, 13–18 April, Vienna, Austria.

Torge, W. 1989. *Gravimetry*. Berlin: de Gruyter.

Tsai, C. H., S. K. Hsu, Y. C. Yeh, C. S. Lee, and K. Y. Xia. 2004. Crustal thinning of the northern continental margin of the South China Sea. *Mar. Geophys. Res.* 25:63–78.

Verdun, J., E. E. Klingele, R. Bayer, M. Cocard, A. Geiger, and H. G. Kahle. 2003. The alpine Swiss-French airborne gravity survey. *Geophys. J. Int.* 152:8–19.

Wei, M., and K. P. Schwarz. 1998. Flight test results from a strapdown airborne gravity system. *J. Geod.* 72:323–332.

Xia, K. Y., C. L. Huang, S. R. Jiang, Y. X. Zhang, D. Q. Su, S. G. Xia, and Z. R. Chen. 1994. Comparison of the tectonics and geophysics of the major structural belts between the northern and southern continental margins of the South China Sea. *Tectonophysics* 235:99–116.

Yale, M. M., D. T. Sandwell, and W. H. F. Smith. 1995. Comparison of along-track resolution of stacked Geosat, ERS 1, and TOPEX satellite altimeters. *J. Geophys. Res.* 100(B8):15117–15127.